Shear strength analysis of interfaces between granular soils and concrete cured under stress

André Luis Meier[1#] 🆔 , Vitor Pereira Faro[1] 🆔 , Edgar Odebrecht[2] 🆔

Article

Keywords
Sand-concrete interface
Curing under stress
Shear strength
Roughness
Bored concrete piles

Abstract
The goal of this study was to improve the understanding of the soil-structure interaction mechanisms at the interface of bored concrete piles cast in sandy soils. In addition, this study aimed to quantify the interface shear strength and identify the factors that influence the response. Roughness measurements and direct shear tests were performed at the interface between two samples of sand (medium and coarse) and concrete cured under stress. The influence of the mean grain diameter, relative density, water content, concrete curing time and normal stress on the interface shear strength were statistically analyzed. The results showed a consistent behavior with the technical literature, but with higher values, which can be attributed to the concrete curing time, a factor not studied by other authors.

1. Introduction

During the execution of bored concrete piles, small displacements can occur along the shaft, which generate shear stresses between pile and soil, called residual stresses (Fellenius & Altaee, 1995). The practical consequence of this phenomenon is inaccurate static load test results, which may result in a higher shaft resistance than the real value and a lower tip resistance (Fellenius, 2020).

Salgado (2008) states that for piles without displacement, the values of the interface friction angle (δ) can be expressed in terms of the critical state friction angle (ϕ'_{cs}) obtained through direct shear tests. Some authors (Lehane et al., 1993; Randolph et al., 1994; Salgado, 2008) found δ values between $0.8\phi'_{cs}$ and ϕ'_{cs} for this type of pile. The explanation for this variation comes from the conditions of pile execution: when well executed, concrete surface roughness tends to be greater than the average diameter of the grains, causing shear to occur in the soil near the pile and not at the interface, which results in a value of δ equal to ϕ'_{cs}. However, in executions with lower quality, the roughness can be reduced, which causes failure to occur at the soil–pile interface, indicating values of δ equal to or smaller than $0.8\phi'_{cs}$.

Ring and direct shear tests are commonly used to estimate the pile axial load capacity through the interface friction angle; nonetheless, the compatibility between laboratory and field conditions needs to be ensured through soil characteristics, surface structures and confinement conditions (Reddy et al., 2000). According to Nardelli et al. (2019), there is a consensus in the technical literature that the interface shear response is mainly influenced by the following conditions: grain characteristics, confining conditions, soil properties, water content, structure surface characteristics and temperature.

The first prominent factor is the roughness on the pile surface. The average roughness (R_a) is one of the most accepted parameters for quantifying surface roughness and is defined as the arithmetic average of the absolute values of the profile height deviations measured from the average line. Another parameter also widely used is maximum roughness (R_{max}), which corresponds to the difference between the highest peak and the lowest valley on a surface (ASME, 2009).

To better evaluate the effects of roughness at a sand-steel interface, Uesugi & Kishida (1986a, b) defined the normalized roughness (R_n) as the ratio of maximum surface roughness to mean grain diameter. In addition, the authors found a bilinear relationship between the normalized roughness and the friction coefficient: first, there is an increase in the friction coefficient with the rise in roughness until the critical point, from which the value becomes constant.

For a sand-concrete interface, Uesugi et al. (1990) observed that the critical point of normalized roughness occurred around the value of 0.1, resulting in a friction coefficient greater than 0.95. Furthermore, based on the normalized roughness value, Paikowsky et al. (1995) defined three categories of surface texture: smooth, for $R_n < 0.02$; intermediate, for $0.02 < R_n < 0.5$; and rough for $R_n > 0.5$.

Regarding the grain characteristics, in soils with subrounded and smooth particles, there is a lower interlock,

#Corresponding author. E-mail address: de.luis.meier@gmail.com
¹Universidade Federal do Paraná, Postgraduate Program in Civil Engineering, Curitiba, PR, Brasil.
²Universidade do Estado de Santa Catarina, Department of Civil Engineering, Joinville, SC, Brasil.

Meier et al., Soil. Rocks, São Paulo, 2023 46(1):e2023004022

1

which allows for rotations during shear. On the other hand, for angular grains, the interlock is higher, increasing the shear strength (Brumund & Leonards, 1973; DeJong & Westgate, 2009).

In interface shear tests, the confining conditions refer to the normal stress applied to the equipment set, which aims to simulate the field characteristics of horizontal stresses. Increasing the normal stress causes an increase in the interface strength due to the decrease in interface dilatancy, which provides a rearrangement of particles within a smaller thickness of the shear zone (Jardine et al., 1993; Dietz & Lings, 2006; Gómez et al., 2008; DeJong & Westgate, 2009; Tiwari & Al-Adhadh, 2014; Tehrani et al., 2016).

Among the soil properties, the main factors affecting the shear strength are the relative density and the mean grain diameter (Uesugi & Kishida, 1986b; Jardine et al., 1993; Dietz & Lings, 2006). At sand-steel interfaces, Uesugi & Kishida (1986b) observed that with the increase in mean grain diameter, the friction coefficient decreased, but with the increase in relative density, the peak value of the friction coefficient increased.

Evaluating the relative density effect in shear stress in rough surfaces, Fakharian & Evgin (1996) observed a hardening behavior in loose sands and a softening behavior in compact sands. For smooth surfaces, a hardening behavior was observed independent of the initial relative density. DeJong & Westgate (2009) noted that dense samples initially presented a contraction and, with the advance of deformations, began to dilate in a zone near the interface.

The loose soils, on the other hand, dilated along the interface shear zone, experiencing, nonetheless, a volume contraction above this region. However, for the postpeak interface shear strength, several authors concluded that it is independent of the initial relative density because the soil had achieved the critical state at the interface (Uesugi & Kishida, 1986b; Jardine et al., 1993; Lehane et al., 1993; Fakharian & Evgin, 1996; Reddy et al., 2000; Dietz & Lings, 2006).

The soil water content, in turn, can be studied in three cases: dry, saturated and unsaturated. Gómez et al. (2008) and Tiwari & Al-Adhadh (2014) observed that the behavior of stress–displacement responses was similar for dry and saturated samples, but dry soil presented higher interface shear strength. Unsaturated soils were investigated by Miller & Hamid (2006) and later by Hamid & Miller (2009), who proposed the use of the shear strength equations, as they noted that the interface strength increases with matric suction, and the linear predictions provide a reasonable model for low suction values, while the nonlinear shear envelope for higher values.

Finally, according to Borges et al. (2020), the concrete curing under stress, as is the case for bored piles, causes an increase in stresses due to thermal expansion, which are relieved, in part, with the thermal shrinkage generated by the drop in temperature. This effect, nonetheless, is more noticeable in large-diameter piles ($D \geq 1$ m) (Pennington, 1995).

At the moment, however, there are no studies in the literature that indicate the effect of concrete curing on the interface shear strength. Therefore, this study aims to improve the understanding of the interaction mechanisms between the soil and concrete surfaces through the influence of the following factors on the behavior of the interface shear strength: mean grain diameter, relative density, water content, normal stress and concrete curing time.

2. Experimental methodology

2.1 Equipment and materials

In the present research, two main pieces of equipment were used: a profilometer and a direct shear apparatus. A Mahr PCV profilometer, shown in Figure 1, was used to measure surface roughness, with a test speed of 0.2 mm/s, which allowed for a shorter scanning time without damaging the sample surface. These measurements provided the primary profile (P-profile), so it was necessary to filter the curve to obtain the roughness profile.

The box of the direct shear equipment, shown in Figure 2, had plan dimensions of 100 mm × 100 mm. The data acquisition, with a frequency of 1.25 Hz, was performed automatically: the displacement measurements were obtained by resistive electronic rulers, while the horizontal force was computed through an S-type load cell.

Two sands were used in this study, named medium and coarse. The soil samples came from the region of Joinville, in the north of the state of Santa Catarina, Brazil, collected by dredging and processing of sand from the Cubatão River. Table 1 shows the properties of the medium sand
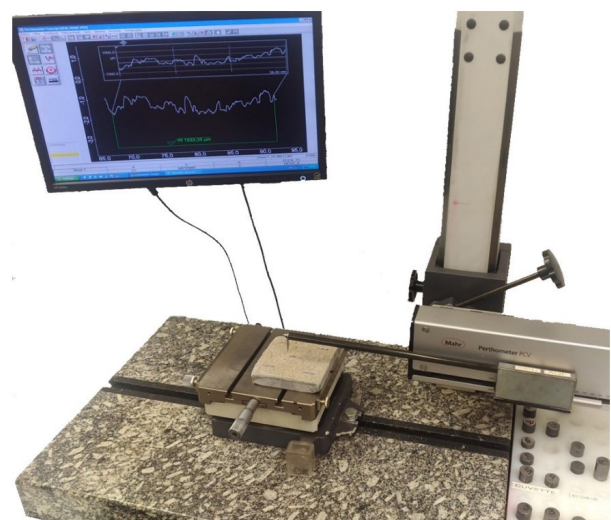

Figure 1. Mahr PCV profilometer.

(D_{50} = 0.60 mm) and coarse sand (D_{50} = 1.10 mm) used in the experimental program. According to the USCS, both soils were classified as poorly graded sand (SP). The grains of both samples were classified as subangular using the criteria prescribed by ASTM D2488 (ASTM, 2017).

The concrete mix used was proposed by Nienov (2016), referring to the piles used in the Araquari Test Site, located near the study area. The materials used were cement CP IV RS, sand (D_{50} = 0.72 mm), gravel (D_{50} = 6.20 mm), water and a superplasticizer admixture. The mixture proportions of the concrete are shown in Table 2. After 28 days, the concrete showed an average uniaxial compressive strength of 35.9 MPa, according to the procedures of ABNT NBR 5739 (ABNT, 2018).

Table 1. Soil characterization.

Description	Medium	Coarse
D_{50} (mm)	0.60	1.10
CU	3.43	5.00
CC	1.06	1.00
G (g/cm³)	2.660	2.649
e_{min} [a]	0.62	0.62
e_{max} [b]	0.79	0.72
Aspect ratio [c]	1.370	1.392
Form factor [d]	0.766	0.761

[a]ABNT NBR 12051 (ABNT, 1991); [b]ABNT NBR 12004 (ABNT, 1990); [c]Aspect ratio = length/width; [d]Form factor = 4π·area/perimeter².

Table 2. Mixture proportion for the concrete (Nienov, 2016).

| Feature or component	Quantity
$f_{ck, min}$ (MPa)	20
$f_{ck, mix}$ (MPa)	35.9
Slump test (cm)	23 +/- 2
Water (kg)	216
Cement CP IV (kg)	415
Sand (kg)	800
Gravel (kg)	870
Superplasticizer (L)	3.0

2.2 Experimental program

The experimental program was divided into two groups: the roughness measurement of concrete specimens cured under stress and the direct shear tests at the sand-concrete interface and of pure sand. First, the independent variables of the study were defined as the mean grain diameter, the relative density of sand, the soil water content, the normal stress and the concrete curing time. However, it should be noted that the concrete curing time was only analyzed in the interface direct shear tests.

The levels of variation of the independent variables were chosen for the following reasons:

- The mean grain diameter the sands should have different granulometries and similarity of the medium sand with the Brazilian normal sand, which is the standardized sand for performing Portland cement compressive strength tests, according to ABNT NBR 7214 (ABNT, 2015);
- The relative density was aimed to include the various levels of density of soils;
- For the water content, a variation of 3% was adopted, equivalent to a 10% change in the saturation of the sand, based on the void ratio;
- For the concrete curing time, a 24 h period was adopted as the maximum feasible time, with the times of 6 h and 18 h being adopted within this interval;
- Finally, for the normal stress, a stress of 180 kPa was obtained as the upper limit of the equipment, and a stress of 100 kPa was considered the center of the set of tests due to its correspondence with the horizontal stresses at approximately 10 m depth in a bored pile.

For the first group of tests, the average roughness (R_a), the maximum roughness (R_{max}) and the normalized roughness (R_n) were the selected responses. The analysis was performed separately for the variables using two statistical methods: crossed and 2k factorial (3rd order). Through the
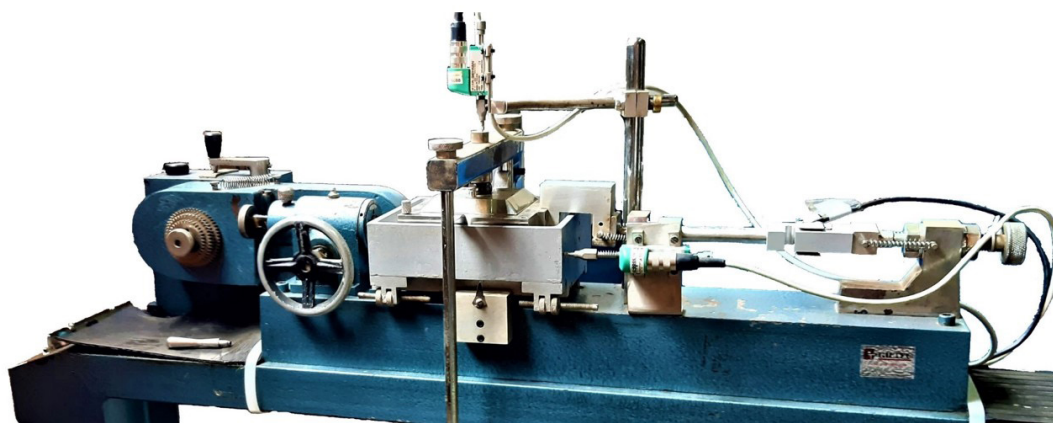
Figure 2. Direct shear apparatus.

crossed factorial method, the influence of grain diameter and normal stress was evaluated; therefore, the relative density was standardized at 70%, and the water content was standardized at 9%. With the 2k factorial method, the aim was to evaluate the effect of grain diameter, relative density and water content on different specimens pressed with the same normal stress of 100 kPa. Sixteen specimens were tested, ten for the cross-factorial stage and eight for the 2k factorial stage.

For the direct shear tests, the response variables were defined as the maximum friction coefficient, called the peak, and the lowest value after the maximum, called the postpeak. The experimental stage used for this group was the crossed factorial method, which allowed obtaining the shear strength parameters through linear regression for different relative densities, water contents, curing times and mean grain diameters. Forty-eight direct shear tests were performed in the sand-concrete interface, and twenty-four tests were performed in pure sand.

2.3 Procedures for interface testing

Figure 3 shows the flowchart for interface testing. After the concrete preparation, it was poured by gravity into the mold (Figure 4A). The surface was then smoothed so that the only roughness came from the impression of the sand on

Figure 3. Flowchart for interface testing.

the specimen. Finally, the mold was deposited in the bottom box of the direct shear equipment (Figure 4B).

The soil samples were first dried in an oven at 105 °C, and the mass of sand was separated for the addition of water until the desired water content was reached for each test. The sand was then compacted inside a ring with a filter (Figure 4C) with the aid of a wooden socket. The compaction control was performed by measuring the mass and water content of the sand inside the mold.

The sample was then extracted from the mold and placed in the upper box of the direct shear equipment (Figure 4D). The total duration of the preparation of each test was approximately 40 minutes. After placing the set in the equipment, the normal stress corresponding to the test was applied. The stabilization period of the vertical displacements was equivalent to the curing time of the concrete, varying, therefore, for each test.

For the roughness measurement tests, this stabilization period was 24 hours, and at the end of this stage, the sample was removed from the equipment, and the sand was cleared away (Figure 4E). Due to the high surface area of the sample, it was chosen to perform 5 roughness readings of 25 mm length per concrete slab cured under stress in the profilometer. The profiles were distributed in different positions on the surface to map the center and sides of each sample. Then, surface metrology software was used to apply a Gaussian filter, with a 2.5 mm cutoff, which generated the roughness profiles and, consequently, the surface roughness parameters.

For the direct shear tests, a shear stress was applied after the stabilization period. After the end of the curing period, a gap was added between the two boxes to avoid breakage of the grains during shear. The total sample displacement was 12 mm, with a shear rate of approximately 0.14 mm/min, resulting in a time to failure of 90 min, higher than the minimum recommended by ASTM D3080 (ASTM, 2011) for the material, but which allowed the next sample to be prepared for testing. At the end of the test, the sheared sample was removed from the equipment (Figure 4F), and its final water content was determined.

3. Analysis and results

The results of this paper were divided into two groups: the surface roughness of concrete specimens cured under stress and the shear strength of the sand-concrete interface and pure sand.

3.1 Surface roughness

The roughness profiles resulting from the measurements in the profilometer are shown in Figure 5, in which it can be seen that the sand with a larger mean grain diameter generates deeper and more frequent peaks and valleys on the concrete surface.

In the crossed factorial analysis, Figure 6a shows the variation in the roughness parameters versus the mean grain
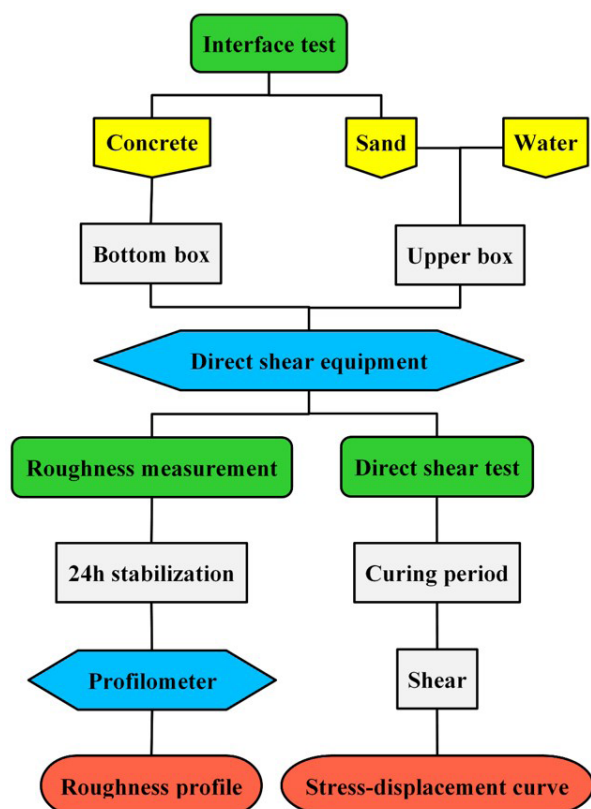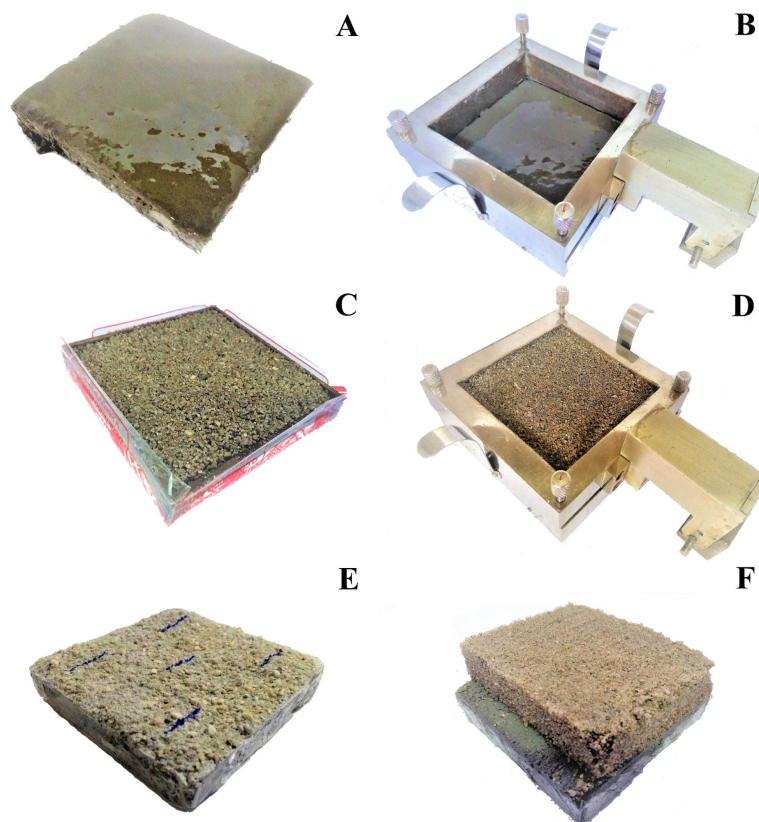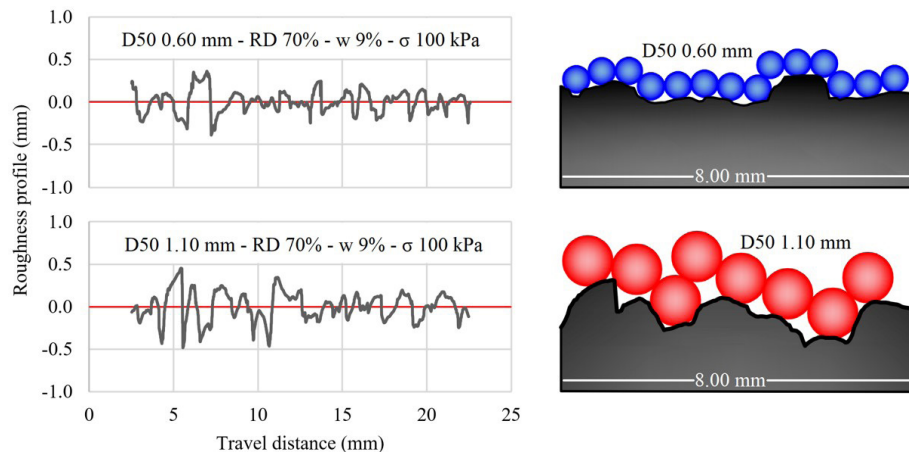
Figure 4. Steps of the interface tests.


Figure 5. Typical roughness profiles.

diameter, in which a small increase in the average roughness (R_a) and a significant increase in the maximum roughness (R_{max}) were observed with increasing grain size. However, the normalized roughness (R_n) decreased as it was inversely proportional to the grain size. For the effect of normal stress, presented in Figure 6b, only small variations of the results around the average were observed, which indicates that, at

this stress level, the variable is not a significant parameter for surface roughness.

Figure 7a shows the 2k factorial analysis for the mean grain diameter, in which the behavior observed for the responses was the same as the crossed factorial analysis, which indicates consistency in the results. It is observed, however, that there is a greater number of outliers. In the
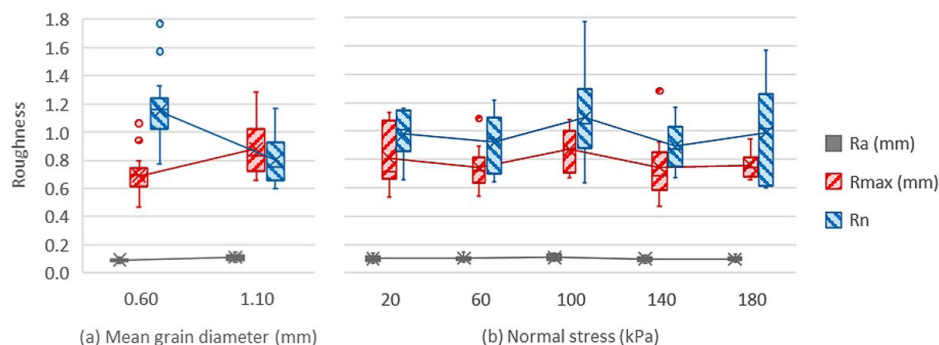
Figure 6. Crossed factorial method: influence of the independent variables on the surface roughness parameters.
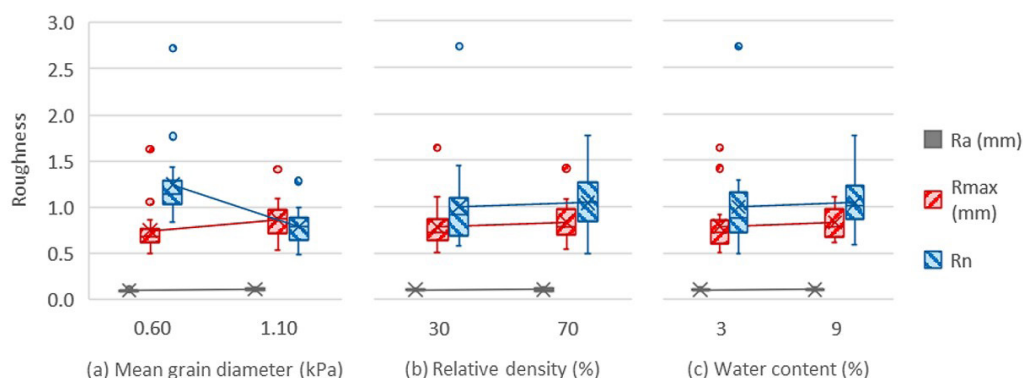
Figure 7. 2k factorial method: influence of the independent variables on the surface roughness parameters.

relative density evaluation (Figure 7b), no variations in the responses were observed, which indicates its noninfluence on the roughness values. A behavior analogous to this is seen in the graph concerning water content (Figure 7c), in which the effect on the test results is also not significant.

Finally, it was concluded that it is possible to assign an average value of the roughness parameters as a function of the mean diameter of the sand grains, without taking into account the variation in the levels of the other independent variables in the present study (normal stress, water content and relative density). Thus, the average values of the parameters for the medium sand (D_{50} = 0.60 mm) are R_a = 0.092 mm, R_{max} = 0.690 mm and R_n = 1.149, while those for the coarse sand (D_{50} = 1.10 mm) are R_a = 0.111 mm, R_{max} = 0.881 mm and R_n = 0.801. Using the criteria defined by Paikowsky et al. (1995), all surfaces were classified as rough, having a value of $R_n > 0.5$.

3.2 Shear strength

The results of the direct shear tests are presented in Figure 8. From the stress–displacement response, a softening behavior can be noted due to the relative density of 70% of the soil. Moreover, the last graphs generated through the test are the vertical displacement versus horizontal displacement, through which it is possible to visualize the initial behavior of contraction, followed by expansion for both cases, agreeing with the definition of softening of the stress–displacement response.

The effect of the mean grain diameter on the friction coefficient is presented in Figure 9a. The general behavior of the friction coefficient is its rise with increasing grain size ($r \approx 0.3$). It is observed, however, that for the postpeak interface shear stress, this factor has practically no influence (r = 0.03), with a nearly horizontal straight line.

A similar behavior was observed in the tests of Nardelli et al. (2019) at sand-concrete interfaces, in which a small increase in (δ/ϕ) values for the peak and postpeak cases occurred with increasing mean grain diameter and decreasing normalized roughness. For the magnitude of the response range of variation, the same influence on the peak shear stress is noticed, whether at the interface or in the sand. This similarity, nonetheless, is not observed in the postpeak tests, whose cause may be related to the dispersion of the sand tests.

The effects of the relative density on the friction coefficient are presented in Figure 9b. First, the shear strength behavior with increasing relative density increases for the interface and sand peak situations, stabilizes at the postpeak interface and decreases for the postpeak sand. The expected behavior,
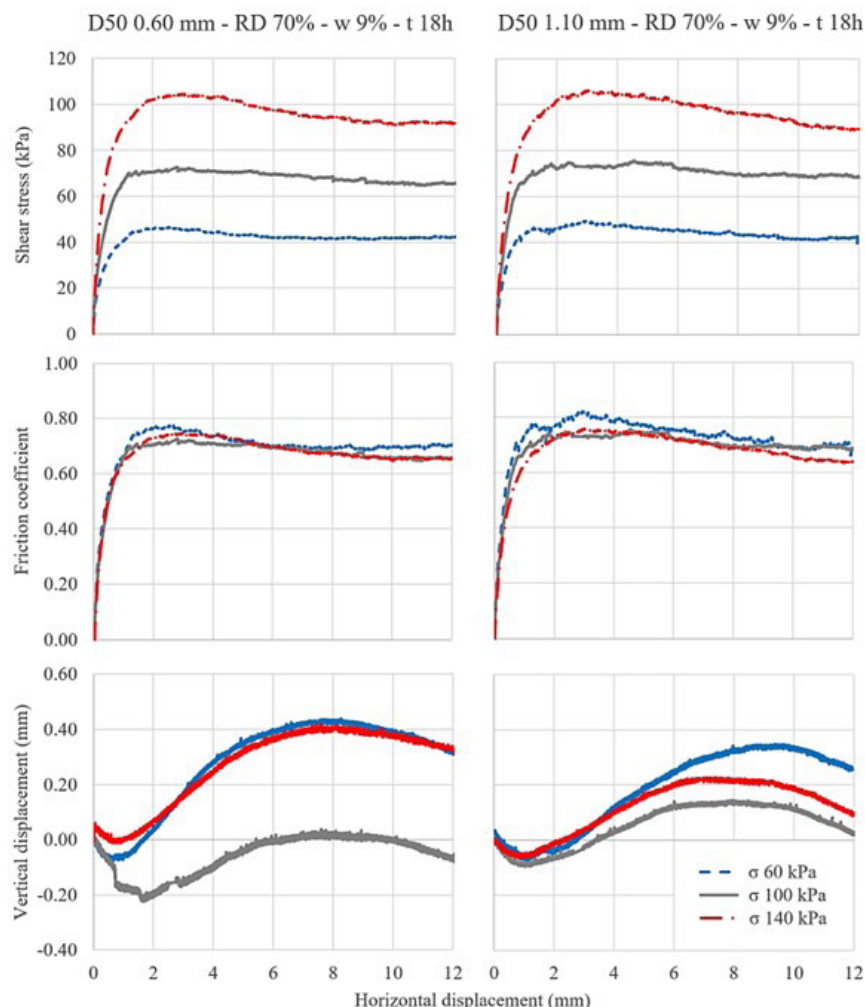
Figure 8. Typical direct shear test results.

according to Uesugi & Kishida (1986b), was that of shear stress rise with increasing relative density for the peak case and no influence in the postpeak. Therefore, it can be stated that there was partial agreement in this case due to the postpeak graph in sand, which despite presenting a decreasing behavior, has an outlier above the upper limit, which indicates the possibility of higher values for the average value.

In the comparison between the interface and sand tests for peak and postpeak stresses, a higher friction coefficient is obtained for the interface case, except for the tests in the postpeak condition with 30% relative density, in which the averages are statistically equal. Finally, regarding the dispersion, there is a similarity in all cases, except for the postpeak tests in sand, for the 70% relative density, in which there is the presence of an outlier, indicating the possibility of greater dispersion of the results, as seen in the graph of the 30% relative density.

The results for the water content evaluation are presented in Figure 9c. The general behavior of the friction coefficient

is its decrease with increasing water content, which is expected according to Tiwari & Al-Adhadh (2014), being present in most cases, with the exception of the sand tests to obtain the peak stress. This variation may have been caused by the soil being partially saturated, which would require a more robust statistical evaluation to precisely define the behavior observed.

Regarding the comparison between the peak and postpeak interface and the sand test, a similar behavior was obtained to the relative density case, with higher average values attributed to the interface analyses. This similarity is also observed in the dispersion of the results, which present narrow size intervals.

The subsequent analysis was the effect of the concrete curing time, as shown in Figure 9d. For this analysis, only the interface test results are considered, as they presented different behaviors for the peak and postpeak cases. A slightly higher peak friction coefficient is perceived with increasing curing time, while for postpeak, a lower value occurs. It is

Meier et al., Soil. Rocks, São Paulo, 2023 46(1):e2023004022

7
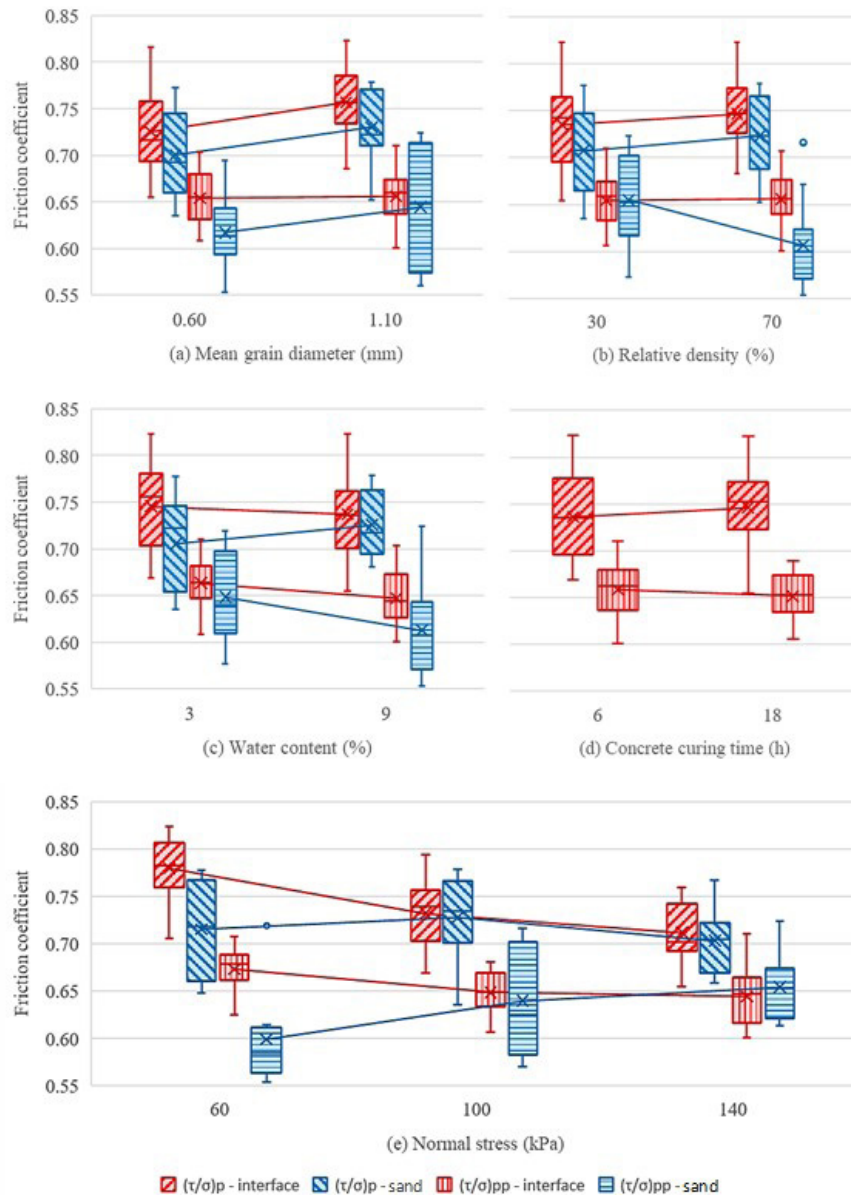
Figure 9. Crossed factorial method: influence of the independent variables on the friction coefficient.

worth mentioning, however, the small numerical difference between the averages for each curing time. Regarding the dispersion of the results, it is observed that the postpeak tests have a smaller variation than the peak tests.

As shown in Figure 9e, the normal stress was studied at 3 actual levels, which allowed a better understanding of the shear strength behavior. First, it is observed that the friction coefficient decreased for the interface tests and increased for the sand tests with increasing normal stress.

Comparing the interface and sand tests for the peak and postpeak stresses, a higher friction coefficient is obtained for the interface case; however, the difference between the averages decreases with increasing normal stress. Finally, regarding the dispersion, a higher accuracy is noticed for

the interface tests in relation to the sand tests, which still present an outlier for the case of the postpeak tests in sand for the normal stress of 60 kPa.

The interface and sand shear strength parameters were also obtained and are presented in Table 3. The Mohr–Coulomb envelope was used for the normal stress levels of 60, 100 and 140 kPa. The values of adhesion (c_a), interface friction angle (δ), soil friction angle (ϕ) and the ratio between interface and soil friction angles (δ/ϕ) were calculated for the peak, indicated by the p-index, and for the postpeak situation, with the pp-index.

From the analysis of the friction angle ratios, it can be noticed, in general, that the postpeak results are higher than the peak ones due to the nonconsideration of adhesion.

Table 3. Shear strength parameters.

D_{50} (mm)	RD (%)	w (%)	t (h)	c_{ap} (kPa)	δ_p	ϕ_p	$(\delta/\phi)_p$	δ_{pp}	ϕ_{pp}	$(\delta/\phi)_{pp}$
0.6	30	3	6	7.78	31.44	33.03	0.95	33.33	32.69	1.02
0.6	30	9	6	8.64	32.31	35.52	0.91	32.16	33.33	0.96
0.6	70	3	6	6.95	32.73	34.69	0.94	33.02	31.64	1.04
0.6	70	9	6	12.68	31.16	35.25	0.88	32.31	30.75	1.05
0.6	30	3	18	6.27	32.92	33.03	1.00	33.18	32.69	1.02
0.6	30	9	18	5.66	31.64	35.52	0.89	32.07	33.33	0.96
0.6	70	3	18	5.41	34.73	34.69	1.00	34.08	31.64	1.08
0.6	70	9	18	1.95	35.97	35.25	1.02	33.06	30.75	1.08
1.1	30	3	6	7.25	35.42	36.23	0.98	34.87	34.55	1.01
1.1	30	9	6	8.50	32.58	36.47	0.89	33.06	34.12	0.97
1.1	70	3	6	9.56	32.30	36.08	0.90	33.48	34.01	0.98
1.1	70	9	6	6.48	33.06	36.16	0.91	31.85	30.88	1.03
1.1	30	3	18	6.02	35.24	36.23	0.97	33.11	34.55	0.96
1.1	30	9	18	8.07	33.54	36.47	0.92	31.79	34.12	0.93
1.1	70	3	18	7.04	34.34	36.08	0.95	32.88	34.01	0.97
1.1	70	9	18	6.04	35.38	36.16	0.98	33.08	30.88	1.07

The adhesion value was chosen to be considered in the peak strength because of the sand grains imprinted on the concrete surface during curing, requiring the breakage of this bond for the displacements to advance. For the postpeak situation, however, there is no physical meaning for the existence of an adhesion parcel; therefore, the average value found was disregarded, and the linear regression line was forced to pass through the origin.

Furthermore, it is noted that the interface friction angle values were very similar, or even higher, than the sand friction angles. This is because the failure studied occurred on a sand–sand surface, as visually observed in the samples after failure, in which high roughness allows a large interlock of the grains and the filling of the surface valleys.

4. Conclusions

The experimental work and the statistical analyses performed throughout this research allowed outlining several considerations on the shear strength of sand-concrete interfaces:

- In the concrete specimens cured under stress, failure occurred at a sand–sand interface due to the high surface roughness, which had valleys filled with sand grains.
- The mean grain diameter was the only relevant factor for the roughness parameters among the variation levels of the independent variables. The relationship between the roughness value and grain size increases for R_a and R_{max} but decreases for R_n.
- The influence of the controllable factors on the friction coefficient was evaluated for the peak and postpeak cases. For the mean grain diameter, the general behavior of the friction coefficient was its rise with increasing particle size, but with low influence on the postpeak interface shear stress. For the relative density, an increasing relation was observed for the interface and sand peak situations but was constant for the interface postpeak case and decreased for the sand postpeak. The variation in the friction coefficient in relation to the water content was also analyzed, which decreased with increasing water content, except for the sand peak case. Regarding the effect of normal stress, a decreasing behavior of the coefficient was observed for the interface tests, and an increase was observed for the sand tests. Finally, a slight increase in the peak friction coefficient is observed due to the effect of the concrete curing time, while for the postpeak, there is a decrease; however, for both cases, the numerical difference is small.
- The results of this study obtained higher values of shear strength parameters than other authors. It is inferred that the cause of this difference is the concrete curing time, a variable not addressed in other studies.

Declaration of interest

The authors have no conflicts of interest to declare. All coauthors have observed and affirmed the contents of the paper, and there is no financial interest to report.

Authors' contributions

André Luis Meier: Conceptualization, Data curation, Formal analysis, Investigation, Methodology, Visualization, Writing – original draft. Vitor Pereira Faro: Conceptualization, Resources, Supervision, Writing – review & editing. Edgar Odebrecht: Conceptualization, Resources, Supervision, Writing – review & editing.

Data availability

The datasets generated during and/or analyzed during the current study are available from the corresponding author on reasonable request.

List of symbols

c_a	Interface adhesion
c_{ap}	Peak interface adhesion
e_{max}	Maximum void ratio
e_{min}	Minimum void ratio
f_{ck}	Characteristic compressive strength
$f_{ck, min}$	Minimum characteristic compressive strength
$f_{ck, mix}$	Characteristic compressive strength of the mixture
r	Correlation coefficient
t	Concrete curing time
w	Water content
CC	Curvature coefficient
CU	Uniformity coefficient
D	Pile diameter
D_{50}	Mean particle diameter
G	Soil particles density
RD	Relative density
R_a	Average roughness
R_{max}	Maximum roughness
R_n	Normalized roughness
δ	Interface friction angle
δ_p	Peak interface friction angle
δ_{pp}	Post peak interface friction angle
δ/ϕ	Interface-soil friction angle ratio
$(\delta/\phi)_p$	Peak interface-soil friction angle ratio
$(\delta/\phi)_{pp}$	Post peak interface-soil friction angle ratio
σ	Normal stress
τ	Shear stress
ϕ	Soil friction angle
ϕ'_c	Critical state friction angle
ϕ_p	Peak soil friction angle
ϕ_{pp}	Post peak soil friction angle

References

ABNT NBR 12004. (1990). *Soil: determination of the maximum index void ratio of cohesionless soils.* ABNT - Associação Brasileira de Normas Técnicas, Rio de Janeiro, RJ (in Portuguese).

ABNT NBR 12051. (1991). *Soil - determination of minimum index void ratio of cohesionless soils - method of test.* ABNT - Associação Brasileira de Normas Técnicas, Rio de Janeiro, RJ (in Portuguese).

ABNT NBR 7214. (2015). *Standard sand for cement tests – specification.* ABNT - Associação Brasileira de Normas Técnicas, Rio de Janeiro, RJ (in Portuguese).

ABNT NBR 5739. (2018). *Concrete - compression test of cylindrical specimens.* ABNT - Associação Brasileira de Normas Técnicas, Rio de Janeiro, RJ (in Portuguese).

ASME B46.1. (2009). *Surface texture: surface roughness, waviness, and lay.* ASME – American Society of Mechanical Engineers, New York.

ASTM D3080. (2011). *Standard test method for direct shear test of soils under consolidated drained conditions.* ASTM International, West Conshohocken, PA. http://dx.doi.org/10.1520/D3080-04.

ASTM D2488. (2017). *Standard practice for description and identification of soils (visual-manual procedures).* ASTM International, West Conshohocken, PA. http://dx.doi.org/10.1520/D2488-17E01.

Borges, A.B., Linn, R.V., Schnaid, F., & Maghous, S. (2020). A simplified numerical approach to the evaluation of residual shaft friction induced by concrete curing in drilled shafts on granular soils. *Revista IBRACON de Estruturas e Materiais*, 13(5), e13505. http://dx.doi.org/10.1590/s1983-41952020000500005.

Brumund, W.F., & Leonards, G.A. (1973). Experimental study of static and dynamic friction between soil and typical construction materials. *Journal of Testing and Evaluation*, 1(2), 162-165. http://dx.doi.org/10.1520/JTE10893J.

DeJong, J.T., & Westgate, Z.J. (2009). Role of initial state, material properties, and confinement condition on local and global soil-structure interface behavior. *Journal of Geotechnical and Geoenvironmental Engineering*, 135(11), 1646-1660. http://dx.doi.org/10.1061/(ASCE)1090-0241(2009)135:11(1646).

Dietz, M.S., & Lings, M.L. (2006). Postpeak strength of interfaces in a stress-dilatancy framework. *Journal of Geotechnical and Geoenvironmental Engineering*, 132(11), 1474-1484. http://dx.doi.org/10.1061/(ASCE)1090-0241(2006)132:11(1474).

Fakharian, K., & Evgin, E. (1996). An automated apparatus for three-dimensional monotonic and cyclic testing of interfaces. *Geotechnical Testing Journal*, 19(1), 22-31. http://dx.doi.org/10.1520/GTJ11404J.

Fellenius, B.H. (2020). *Basics of foundation design.* Retrieved in April 19, 2022, from www.fellenius.net

Fellenius, B.H., & Altaee, A.A. (1995). Critical depth: how it came into being and why it does not exist. *Proceedings of the Institution of Civil Engineers - Geotechnical Engineering*, 113(2), 107-111. http://dx.doi.org/10.1680/igeng.1995.27590.

Gómez, J.E., Filz, G.M., Ebeling, R.M., & Dove, J.E. (2008). Sand-to-concrete interface response to complex load paths in a large displacement shear box. *Geotechnical Testing Journal*, 31(4), 358-369. http://dx.doi.org/10.1520/GTJ100220.

Hamid, T.B., & Miller, G.A. (2009). Shear strength of unsaturated soil interfaces. *Canadian Geotechnical Journal*, 46(5), 595-606. http://dx.doi.org/10.1139/T09-002.

Jardine, R.J., Lehane, B.M., & Everton, S.J. (1993). Friction coefficients for piles in sands and silts. In D.A. Ardus, D. Clare, A. Hill, R. Hobbs, R.J. Jardine & J.M. Squire (Eds.), *Offshore site investigation and foundation behavior* (Advances in Underwater Technology, Ocean Science and Offshore Engineering, Vol. 28, pp. 661-677). London: Springer. http://dx.doi.org/10.1007/978-94-017-2473-9_31.

Lehane, B.M., Jardine, R.J., Bond, A.J., & Frank, R. (1993). Mechanisms of shaft friction in sand from instrumented pile tests. *Journal of Geotechnical Engineering*, 119(1), 19-35. http://dx.doi.org/10.1061/(ASCE)0733-9410(1993)119:1(19).

Miller, G.A., & Hamid, T.B. (2006). Interface direct shear testing of unsaturated soil. *Geotechnical Testing Journal*, 30(3), 13301. http://dx.doi.org/10.1520/GTJ13301.

Nardelli, A., Cacciari, P.P., & Futai, M.M. (2019). Sand-concrete interface response: the role of surface texture and confinement conditions. *Soil and Foundation*, 59(6), 1675-1694. http://dx.doi.org/10.1016/j.sandf.2019.05.013.

Nienov, F.A. (2016). *Bored pile performance of large diameter in sandy soil under vertical load* [Doctoral thesis, Federal University of Rio Grande do Sul]. Federal University of Rio Grande do Sul's repository (in Portuguese). Retrieved in April 19, 2022, from http://hdl.handle.net/10183/150506

Paikowsky, S.G., Player, C.M., & Connors, P.J. (1995). A dual interface apparatus for testing unrestricted friction of soil along solid surfaces. *Geotechnical Testing Journal*, 18(2), 168-193. http://dx.doi.org/10.1520/GTJ10320J.

Pennington, D.S. (1995). Cracked? Exploring postconstruction evidence in the interpretation of trial pile data. *Geotechnical Engineering*, 113(3), 132-143. http://dx.doi.org/10.1680/igeng.1995.27809.

Randolph, M.F., Dolwin, J., & Beck, R. (1994). Design of driven piles in sand. *Geotechnique*, 44(3), 427-448. http://dx.doi.org/10.1680/geot.1994.44.3.427.

Reddy, E.S., Chapman, D.N., & Sastry, V.V.R.N. (2000). Direct shear interface test for shaft capacity of piles in sand. *Geotechnical Testing Journal*, 23(2), 199-205. http://dx.doi.org/10.1520/GTJ11044J.

Salgado, R. (2008). *The engineering of foundations*. Boston: McGraw-Hill.

Tehrani, F.S., Han, F., Salgado, R., Prezzi, M., Tovar, R.D., & Castro, A.G. (2016). Effect of surface roughness on the shaft resistance of nondisplacement piles embedded in sand. *Geotechnique*, 66(5), 386-400. http://dx.doi.org/10.1680/jgeot.15.P.007.

Tiwari, B., & Al-Adhadh, A.R. (2014). Influence of relative density on static soil-structure frictional resistance of dry and saturated sand. *Geotechnical and Geological Engineering*, 32(2), 411-427. http://dx.doi.org/10.1007/s10706-013-9723-6.

Uesugi, M., & Kishida, H. (1986a). Influential factors of friction between steel and dry sands. *Soil and Foundation*, 26(2), 33-46. http://dx.doi.org/10.3208/sandf1972.26.2_33.

Uesugi, M., & Kishida, H. (1986b). Frictional resistance at yield between dry sand and mild steel. *Soil and Foundation*, 26(4), 139-149. http://dx.doi.org/10.3208/sandf1972.26.4_139.

Uesugi, M., Kishida, H., & Uchikawa, Y. (1990). Friction between dry sand concrete under monotonic and repeated loading. *Soil and Foundation*, 30(1), 115-128. http://dx.doi.org/10.3208/sandf1972.30.115.